Combined Pulse Data Transmission and Indoor Localization Using 60-GHz-UWB MMIC Technology

CHRISTOPHE LOYEZ[1,2] (Member, IEEE), **MICHAEL BOCQUET**[1,2], **NATHALIE ROLLAND**[1,2], **AND KAMEL HADDADI**[1,2] (Member, IEEE)

[1]Institut d'Electronique, de Microélectronique et de Nanotechnologies, Université de Lille, CNRS, Université Polytechnique Hauts-de-France, UMR 8520-IEMN, 59000 Lille, France
[2]IRCICA, USR CNRS 3380, 59652 Villeneuve-d'Ascq, France

CORRESPONDING AUTHOR: K. HADDADI (e-mail: kamel.haddadi@ieee.org)

ABSTRACT This article presents a pulse radio transmission system operating in the millimeter-wave regime for simultaneous binary information transmission and location in an intrabuilding environment. In particular, the location solution mutualizes the hardware architectures of three sensors of known position to extract the location information of a sensor entering their vicinity and, thus, uses the radio communication signals to extract this location information. Experimental validation considering the 60-GHz transceiver designed and realized on pseudomorphic high electron mobility transistor (pHEMT) technology is exemplary shown with localization error quantified to 16 cm.

INDEX TERMS Impulse system, millimeter wave, pseudomorphic high electron mobility transistor (pHEMT), time difference of arrival (TDOA), ultrawide band (UWB).

I. INTRODUCTION

LOCATION devices are becoming more and more common in our daily environment with different performance requirements depending on the application [1], [2], [3], [4], [5]. Location can be a mechanism to optimize network connectivity while minimizing the energy consumed by the network sensors. Global positioning system (GPS)-type solutions meet most of these requirements but suffer from a loss of efficiency in intrabuilding environments. The deployment of specific infrastructures for the location function in an intrabuilding environment remains limited. The development of radio communication systems brings innovations that allow reliable communications while being mobile. In these mobile ad hoc networks (MANETS), network connectivity is one of the key requirements for quality communication [6]. In many cases, the information routing protocols are based on the location information of the access points as well as the mobile terminals. In this context, communication and location functionalities are expected to be increasingly intertwined. With the advent of devices that combine different functionalities, we [7], [8], [9], [10] and others [11], [12], [13], [14] have contributed

to the implementation of this intrabuilding location without requiring heavy infrastructures.

The study described in this article is in line with the growing need for interoperable systems capable of providing several radio-frequency functions simultaneously for intrabuilding communication and location applications. The location process avoids the use of the beacon that requires infrastructure deployment. In particular, dedicated sensors of the ad hoc network assume themselves the role of spatial references. Thus, no specific infrastructure is required for this new solution. Moreover, the location process allows to extract the location information directly from the pulse signal on which the binary information is grafted. The system architecture thus makes it possible to simultaneously ensure the functions of communication and location. In contrast with commercial systems based on relatively complex modulation schemes, we developed a binary transceiver that has the best compromise between data rate and positioning accuracy. In particular, the ratio On/Off is related to two states: 1) transmission of the signal and 2) no transmission. The ON–OFF keying (OOK) modulation used during transmission is carried out in a direct modulation mode: the binary

information signal is used to power or not the entire transmitter device, including the oscillator. This gives a very high On/Off ratio compared to transmitters using external modulation. In addition, in conventional architectures, all three sensors are connected using external wiring. In the proposed architecture, two of the sensors received the source signal and repeat it through a second emitting antenna: their specific task is to record the input signal and transmit it to the third sensor. This latter receives both source signal and those emitted by each of the other sensor. This versatile architecture allows to consider a wide range of experimental scenarios with different *X* and *Y* positions of the sensors. It has to be mentioned that this technique requires the exact spatial knowledge of the three sensors.

The synthesis of the results of this study is divided in three sections. Section II describes the pulse data transmission system that has been realized as well as its performance and characteristics. Section III details how the localization functionality is implemented in the architecture of the radio communication system. Section IV deals with the experimentally established results and makes the assessment on the system constraints presented in the previous sections.

II. MILLIMETRE-WAVE UWB TRANSCEIVER

This millimeter-wave transceiver is designed to transmit ultrawide band (UWB) impulse signals with pulse width in the range of 300–400 ps. The novelty of the proposed approach concerns the energy that is consumed only during the transmission of frequency up-converted pulses at 60 GHz. The 60-GHz frequency band is chosen because of its vast amount of spectral resources which are not regulated to -41 dBm/MHz such as for the conventional UWB frequency band [15]. Another advantage of the 60-GHz frequency band is the size reduction of the antennas and of the overall system [16]. The monolithic microwave-integrated circuit (MMIC) technology employed is based on pseudomorphic high electron mobility transistors (pHEMTs) with transition frequencies f_T up to 120 GHz. Transmission lines and stubs are designed in microstrip technology. The MMIC chip is connected to an external alumina microstrip line ended by a coaxial V-band patch antenna having a 60° beamwidth. The antenna has not been integrated to limit the MMIC size.

A. MILLIMETRE-WAVE RF TRANSMITTER

The architecture of the Tx transmitter consists essentially of a voltage-controlled oscillator (VCO) associated to a medium power amplifier (MPA) as described in Fig. 1. The oscillator is designed on the basis of a negative differential resistance (NDR). This NDR is achieved by means of a normally-on transistor (labeled N1 on Fig. 1). To make it unstable in the frequency range around 60 GHz, this 4×65 μm^2 transistor is fed back through the gate using a 600-μm stub ended by a short circuit. In this configuration, the impedance seen by the source access of N1 is close to an open circuit which fulfils the oscillation conditions when the voltage VS1 equals
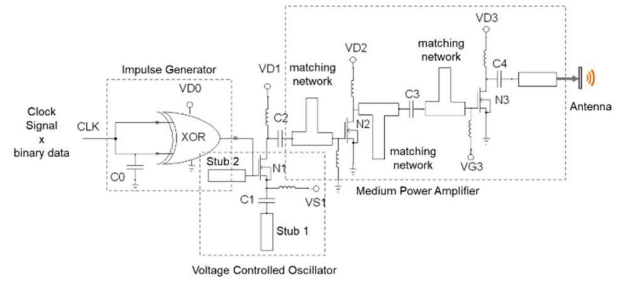

FIGURE 1. 60-GHz Tx schematic.

0.65 V. The average signal power delivered by this oscillator is slightly above 0 dBm. Following the NDR, a two-stage MPA is cascaded: the first stage has two roles. First, it acts as a buffer that reduces the pulling effect that the NDR could suffer. This buffer consists of the N2 transistor mounted as a common source. Its role is to optimize the power of the signal delivered by the NDR under load conditions close to 50 Ω at the frequency of 60 GHz. The matching network consists of a transmission line backed by a stub ended by an open circuit. The design of these matching networks also aims to boost the power gain of the overall.

The actuation of the RDN oscillator is performed by impulse signals applied to the gate access of the N1 transistor. The impulse signals are provided by an integrated generator: the main principle of this pulse generator is based on a fast XOR gate associated with a capacitive element inducing the expected delay. As depicted in Fig. 1, the clock signal is connected directly to one of the inputs of the XOR gate. The delayed clock signal is applied to the second port: the delay results from the capacitance C0 of a varactor diode whose capacitance value is tunable by a supply voltage. By the way, this topology enables to tune the pulse width. The pulse repetition depends on the clock frequency and can be adapted in the typical range 330 ps–1 μs.

In the use case presented, the pulses perform a direct amplitude modulation of the millimeter waveform by inhibiting or not the NDR oscillator operation depending on whether or not a pulse is generated. Because it is based on an amplitude modulation technique, this transmitter can perfectly well make do with a local oscillator with degraded phase noise properties. Thus, this amplitude modulation causes a frequency upconversion of the pulse signals delivered by the integrated generator. The clock signal feeds the oscillator only when a "1" symbol is transmitted: depending on the clock frequency, a greater or lesser number of pulses will be transmitted, depending on the symbol duration. No pulse is transmitted in the case of a "0" symbol because the clock signal is inhibited in this case. Thus, the clock signal triggers pulses only when a 1 symbol is transmitted. The operation which consists in activating a clock signal only when a symbol 1 contained in a pseudo-random sequence is transmitted is carried out with the help of the data timing generator (Tektronix DTG 5334). The maximum power at the output of the transmitter is equal to 10 dBm.
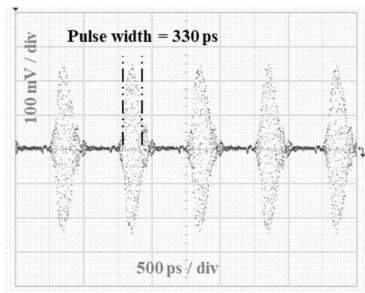
(a)
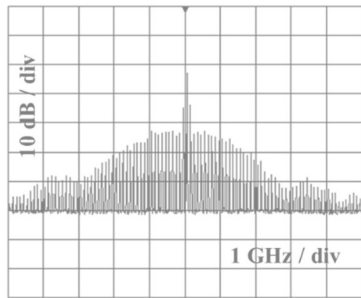
(b)

FIGURE 2. (a) Waveform signal at the 60-GHz Tx output measured using a Keysight Infinium DCA-J 86100 Digital Scope (70-GHz bandwidth). (b) Spectrum of the 60-GHz Tx signal—fo = 60 GHz.
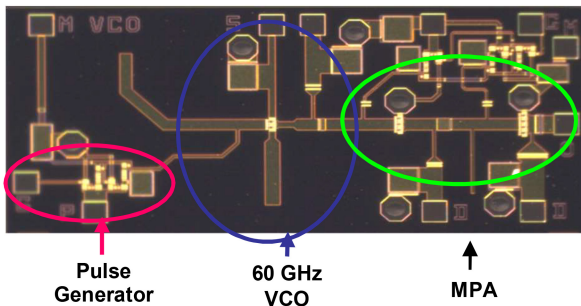

FIGURE 3. MMIC achievement of the TX—Die size: 0.8 x 1.9 mm².

TABLE 1. List of dc supply voltages.

VD0	VS1	VD1	VD2	VD3
2.5 V	0.65 V	2.5 V	2.5 V	3 V

The measured power added efficiency of the Tx is 3.5% during the continuous emission of a sinusoidal signal with a 60-GHz center frequency. Fig. 2(a) shows a measured waveform of the 60-GHz impulse signals generated by the Tx and Fig. 2(b) shows the related spectrum.

The frequency bandwidth of the transmitter is equal to 3 GHz so that the pulse width is optimal for the value of 330 ps. The test data rate reaches up to 100 Mbits/s. A micrograph of this transmitter is shown in Fig. 3 and the TX specifications are summarized in Tables 1 and 2.

B. 60-GHZ RECEIVER

The 60-GHz reception chain described Fig. 4 is based on the quadratic detection of the propagated signals. Thus, the

TABLE 2. List of transistor widths (in μm) and capacitor values.

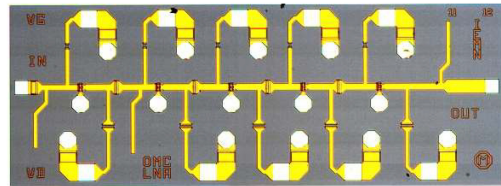| N1	N2	N3	C1	C2	C3
4 x 25	6 x 25	8 x 25	1 pF	2.5 pF	1.5 pF

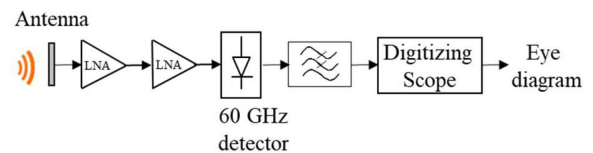**FIGURE 4.** Micrograph of the 60-GHz LNA (1 × 3 mm²).

FIGURE 5. 60-GHz receiver architecture.

phase noise of the local oscillator does not affect the integrity of the communication This also minimizes the number of components involved in the receiver. Indeed, the front-end of the receiver only includes a chain of low noise amplifiers (LNAs) followed by an envelope detector. The architecture of the LNA is based on a cascading of transistors mounted in a common source. The matching networks between the different stages are optimized to extract an optimal compromise between the gain, noise, and stability of the amplifier and its footprint. Indeed, this last point remains crucial if one wishes to cascade several of these amplifiers without causing parasitic oscillations in the reception chain. This is all the more difficult to achieve, as the receiving antenna does not have an impedance of 50 Ohm in the whole frequency band for which the amplifier has a gain greater than 1. In order to be able to cascade these amplifiers during a transfer to a ceramic box, a fine analysis of the stability was carried out on the basis of the normalized determinant function (NDF) method [17].

The five stages of this LNA are composed by a pHEMT mounted as a common source with a 4×15 um gate width. It provides a power gain of 27 dB over the 57–60-GHz frequency band. The noise figure of this amplifier was measured at 60 GHz, for which it has a value of 5.2 dB. After this low noise amplification, the envelope of the amplified signal is obtained by detection. This envelope separation operation involves a RF detector [9] with a sensitivity of 1.6 mV per μW at 60 GHz.

The global architecture of the receiver is depicted in Fig. 5.

C. EXPERIMENTAL RESULTS IN COMMUNICATION RELIABILITY

The downside of such a simplified architecture is that it only allows the use of weak energy-efficient modulation
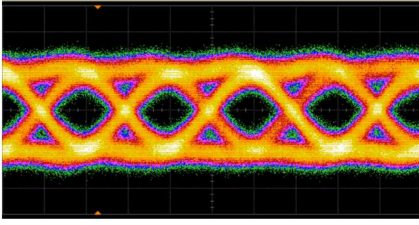
FIGURE 6. Eye diagram of the received signal after filtering (D = 100 Mpbs—duty cycle = 50% – range = 5 m).
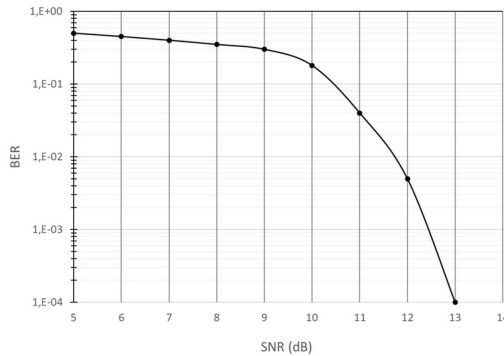

FIGURE 7. BER as a function of the SNR (D = 100 Mb/s).

FIGURE 8. Illustration of the global location scenario.

schemes such as OOK. However, it remains compatible with radio transmissions over distances of a few meters, typical of communications in indoor environments. In order to validate the link reliability, a data transmission is achieved using an OOK modulation scheme with a data rate of 100 Mbit/s. The test bench is composed by the transmitter and receiver described in the previous section. For a range of 5 m, the eye diagram is recorded using a Keysight Infinium scope DSO1204A and shown in Fig. 6.

Using a logic analysis system (Keysight 16903A), the bit error rate (BER) of the transmitted signals is measured offline as a function of the signal-to-noise ratio (SNR).

By tuning the Tx power, the BER of the transmitted signal is evaluated as a function of SNR as described in Fig. 7. Although the OOK modulation scheme has a lower energy efficiency, the hardware configuration of the developed solution enables to reach BER of the order of 10^{-4} for a SNR of 13 dB that relates to a transmission range of approximately 10 m with respect to the system parameters.

III. DISTRIBUTED LOCALIZATION DEVICES
A. MEASUREMENT PRINCIPLE
The various communicating objects equipped with this transceiver can thus communicate between them different types of digital data, whether they are dedicated to the payload or to the routing protocols, including information about their location.

The context of our study consists of a mesh network of cooperative wireless sensors. Among them, three sensors called anchors mutualize their hardware architectures in order to estimate the location of the transmitter (Tx) arriving
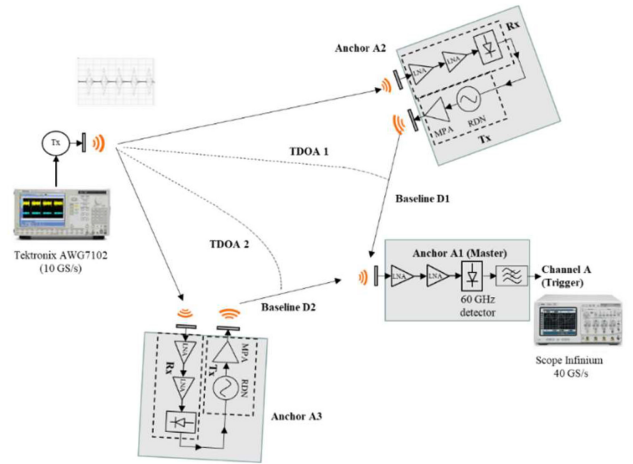
in the localization area. These three anchors, labeled A1, A2, and A3, work in pairs. By organizing the three sensors into pairs, it is possible to extract two time difference-of-arrival (TDOA) values. The main anchor (labeled A1 in Fig. 8) is common to both pairs (A1;A2) and (A1;A3). Each of the pairs is used to determine a (TDOA$_1$ and TDOA$_2$, respectively). The set of possible source locations for each TDOA value corresponds geometrically to a hyperbola. The Tx location is estimated by the intersection of two hyperbolas, each related to one of the measured TDOA values.

One of the anchors (A2 or A3 in turn) acts as a repeater, relaying the pulse signal from the source to be located to the master anchor A1. Then, the master receives both source signal and those emitted by each of the sensor A2 and A3. As the locations of the anchors are known, the travel time between each anchor can be determined and subtracted from the TDOA measured using a digital scope. As the pulse signal retransmitted by a repeater has a power in the order of 10 dBm, it has been found that reflected signals (parasitic signals) remain at much lower amplitudes.

The overall topology is described in Fig. 8: the transmitter, whose location is to be estimated, enters the direct path of the other sensors by emitting pulsed signals at 60 GHz as described above. These signals are then received by A1, A2, and A3. As mentioned previously, only one anchor A2 then A3 repeats the signals to the master anchor A1.

Potentially, the location accuracy depends closely on the pulse width but also on the distance between the two antennas collecting the signals involved in the TDOA measurement. At a minimum, this distance called the baseline must be greater than the product $c.T$ (i.e., 10 cm) where T corresponds to the pulse width (T=330 ps). In order to prevent the phenomenon of geometric dilution of the localization precision (Fig. 9), it is recommended to consider a baseline value as large as possible, usually at least ten times the minimum value (i.e., 1 m). The possibility of relaying the pulse signal via a repeater is an advantage for fulfilling this requirement without using cables.
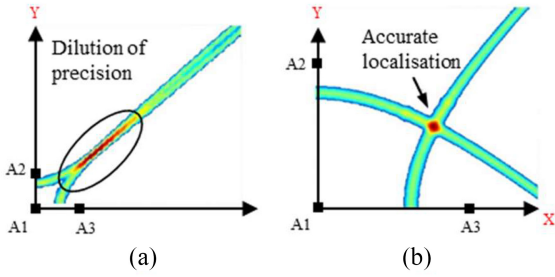
FIGURE 9. Illustration of the estimated location from the intersection of the hyperbolas corresponding to the TDOA values. (a) Baseline = 10 cm. (b) Baseline = 1 m.

FIGURE 10. Location error (m) versus radial distance.

B. THEORY

The system of equations modeling the possible solutions of the Tx location as a function of the $TDOA_1$ and $TDOA_2$ values can be solved using the Chan approach [18]. If we consider R1, R2, and R3 the respective distances between the location A (X, Y) of the Tx to be estimated and the anchors A1 (X_1, Y_1), A2 (X_2, Y_2), and A3 (X_3, Y_3) involved in the location process, the estimated coordinates (X,Y) of Tx are obtained by solving (1)–(3)

$$\begin{bmatrix} X \\ Y \end{bmatrix} = -\begin{bmatrix} X_{2,1} & Y_{2,1} \\ X_{3,1} & Y_{3,1} \end{bmatrix}^{-1}$$
$$* \left\{ \begin{bmatrix} R_{2,1} \\ R_{3,1} \end{bmatrix} R_1 + \frac{1}{2} \begin{bmatrix} R_{2,1}^2 - K_2 + K_1 \\ R_{3,1}^2 - K_3 + K_1 \end{bmatrix} \right\} \quad (1)$$

with

$$R_{i,1}^2 + R_{i,1}R_1 = K_i - K_1 - 2X_{i,1}X - 2Z_{i,1}Z \quad (2)$$
$$R_1 = R_1(X, Y) = \left[(X_1 - X)^2 + (Y_1 - Y)^2 \right]^{1/2} \quad (3)$$

where

$$K_1 = X_1^2 + Y_1^2 + Z_1^2, \quad K_2 = X_2^2 + Y_2^2 + Z_2^2,$$
$$K_3 = X_3^2 + Y_3^2 + Z_3^2,$$
$$X_{2,1} = X_2 - X_1, \quad X_{3,1} = X_3 - X_1, \quad Y_{2,1} = Y_2 - Y_1,$$
$$Y_{3,1} = Y_3 - Y_1$$

and $R_{2,1} = TDOA_{1.c}$, $R_{3,1} = TDOA_{2.c}$.

C. EXPERIMENTAL RESULTS

The location process described above is submitted to experimental validation in an indoor environment consisting of a room of dimensions 7×5 m^2, furnished with metal and wood cabinets and furniture. The three anchors forming an orthogonal frame of reference are placed in the room in such a way as to direct their antennas toward the whole room in which the location of the Tx source will evolve. In a first configuration, the three sensors are arranged equidistantly on two perpendicular axes as shown in Fig. 8. Thus, we performed the first measurements considering baselines of values equal to 3 m for the different pairs. As can be seen from the results shown in Fig. 10, the location
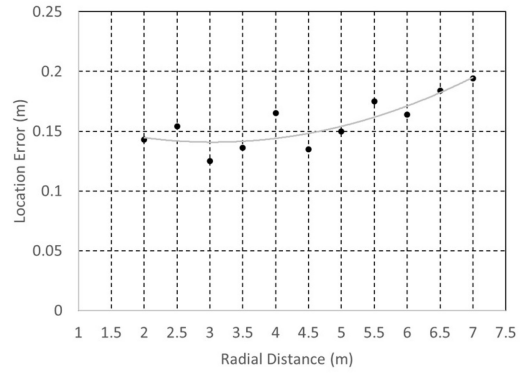

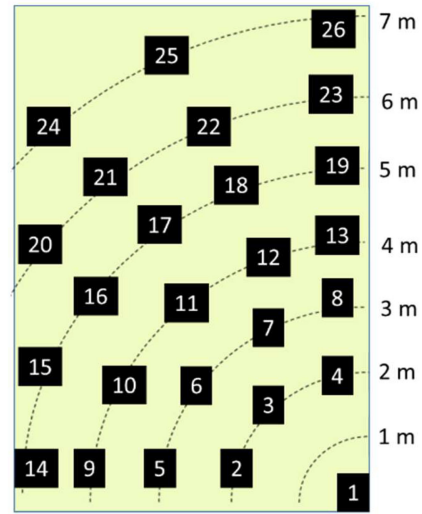**FIGURE 11.** Illustration of the environment (room size = 5 × 7 × 2.5 m³) listing locations considered for the experimental evaluation.

error tends to deteriorate with the increase of the radial distance.

In such an experimental setup, the location error is mainly driven by the pulse width (330 ps) which is translated by a minimum spatial error of 10 cm. The sampling frequency of the analyzed signal is also a key parameter: at 10 gigasamples per second, the sampling step is 100 ps, which corresponds to an additional step difference of more than 3 cm that weight the localization error. These results remain unchanged whether the OOK modulation is active or not. Indeed, the principle of TDOA is transparent whether the pulses are periodic or not. These results validate the simultaneous multifunctionality of the solution developed in this study since the location process is performed from the impulse signal carrying the binary data.

The measurement environment is a furnished room (5 × 7 × 2.5 m³) comprises mainly five tables (wood) with 12 chairs (metals) with conventional computers (screens, keyboards, . . .). The walls are in plywood. In order to examine the performance of the developed device in a more realistic way, the locations of both the source and the anchors
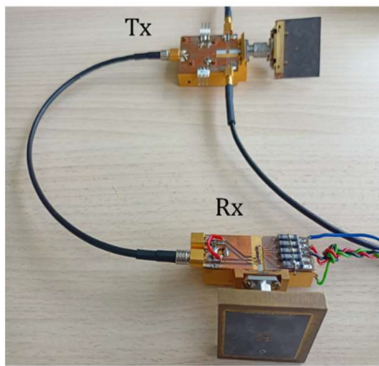
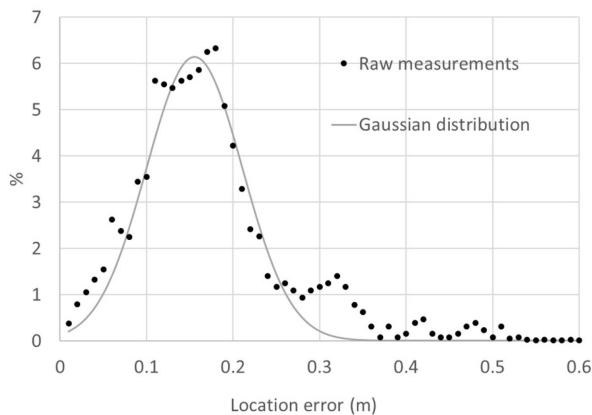**FIGURE 12.** Photograph of an anchor including Tx/Rx modules.

FIGURE 13. Distribution function of the experimental location errors.

frequency of the analyzed signals is a parameter that also affects the location performance. Typically, the location error remains within a bound corresponding to twice this minimum observed value. The disadvantage remains the need to sample these pulses after detection, which requires fast samplers.

IV. CONCLUSION

To address the growing need of compact devices for communication and location in an indoor environment, an integrated dedicated pulse radio transmission system has been designed and fabricated in monolithic integrated technology. To achieve a high compact solution, UWB signals are transposed to the millimeter-wave regime at 60 GHz. The chip can address simultaneous binary information transmission and location in intrabuilding environment with measurement error of 16 cm, quantified through more than 400 experimental configurations considered for TDOA measurements. The impact of the Z-position of the Tx on the location error is relatively small if the Z-position varies within one meter. This has been verified qualitatively, but quantitative data has not been extracted as it is beyond the scope of this procedure. In particular, we verified that the error is greatly reduced when the anchors are spaced further apart.

Such a system can work with more fix anchors. Even if the scalability has not been the main objective of this preliminary work, one perspective will be to study the scalability in regard with the additional complexity of the overall solution and related performance (location accuracy, full spatial 2-D or 3-D coverage, ...).

Regarding the frequency, around 60 GHz, line of sight is indeed the predominant signal for which no specific problems have been encountered. Indeed, if there is an obstruction, more sensors can be definitively useful. Regarding the algorithm modification, the analytical modeling considered two pairs of TDOA and, consequently, the direct and simplest idea should be directed toward the use of the same algorithm but with different anchors.

are then modified to successively cover the different areas of the room. Fig. 11 shows the configuration of the room used for the measurements with the locations taken into consideration for the different sensors. A photograph of an anchor including the modules Tx/Rx is presented Fig. 12. For each configuration tested, each anchor occupies one of 26 possible locations. The source to be located then occupies successively the 23 remaining locations. Once the 23 estimates are made, the locations of the three anchors are then modified. This leads to a large number of measurements since 26 locations are listed homogeneously in this room.

As mentioned earlier, patch antennas with a 3-dB aperture of the order of $+/- 60°$ are used. During TDOA measurements, the antennas of the transmitter to be located and those of the sensors are facing each other in order to ensure a radio link under line of sight conditions. More than 400 configurations are thus considered for TDOA measurements: for each of them, the localization error is experimentally determined. To synthesize these results, their distribution function is shown in Fig. 13. This distribution can be approximated by a Gaussian function with a mean value of 16 cm and a standard deviation of 5.5 cm

These experimental results demonstrate that the location error is mostly close to the spatial resolution associated with the 330-ps pulse width, i.e., 10 cm. The sampling

REFERENCES

[1] S. Sadowski and P. Spachos, "RSSI-based indoor localization with the Internet of Things," *IEEE Access*, vol. 6, pp. 30149–30161, 2018, doi: 10.1109/ACCESS.2018.2843325.

[2] Z. Abu-Shaban, H. Wymeersch, T. Abhayapala, and G. Seco-Granados, "Single-Anchor two-way localization bounds for 5G mmWave systems," *IEEE Trans. Veh. Technol.*, vol. 69, no. 6, pp. 6388–6400, Jun. 2020.

[3] J. Palacios, G. Bielsa, P. Casari, and J. Widmer, "Single- and multiple-access point indoor localization for millimeter-wave networks," *IEEE Trans. Wireless Commun.*, vol. 18, no. 3, pp. 1927–1942, Mar. 2019.

[4] E. Grossi, M. Lops, and L. Venturino, "Adaptive detection and localization exploiting the IEEE 802.11ad standard," *IEEE Trans. Wireless Commun.*, vol. 19, no. 7, pp. 4394–4407, Jul. 2020.

[5] G. Lee, H. Koh, U.-S. Suh, and T. W. Kim, "An IR-UWB angle-of-arrival sensor IC using auto-toggled time-to-digital converter," *IEEE Microw. Wireless Compon. Lett.*, vol. 29, no. 11, pp. 749–752, Nov. 2019.

[6] M. Tubaishat and S. Madria, "Sensor networks: An overview," *IEEE Potentials*, vol. 22, no. 2, pp. 20–23, Apr./May 2003, doi: 10.1109/MP.2003.1197877.

[7] C. Loyez, M. Bocquet, and K. Haddadi, "Six-port technology for 5G millimeter-wave localization systems," in *Proc. Int. Conf. Electromagn. Adv. Appl. (ICEAA)*, 2018, pp. 272–275, doi: 10.1109/ICEAA.2018.8520353.

[8] C. Loyez, M. Bocquet, and K. Haddadi, "A 60-GHz six-port system for localization based on time difference of arrival," in *Proc. IEEE Radio Wireless Symp. (RWS)*, 2019, pp. 1–4, doi: 10.1109/RWS.2019.8714390.

[9] M. Bocquet, C. Loyez, and K. Haddadi, "Quadratic detection-based millimeter-wave MMIC for TDoA and AoA measurement," in *Proc. Int. Conf. Electromagn. Adv. Appl. (ICEAA)*, 2021, pp. 321–324, doi: 10.1109/ICEAA52647.2021.9539767.

[10] C. Loyez, M. Bocquet, and K. Haddadi, "MMIC vector topology enabling multi RF functionalities for 5G and beyond," *IEEE Access*, vol. 9, pp. 114418–114427, 2021, doi: 10.1109/ACCESS.2021.3098179.

[11] J. Xia, C. L. Law, Y. Zhou, and K. S. Koh, "3–5 GHz UWB impulse radio transmitter and receiver MMIC optimized for long range precision wireless sensor networks," *IEEE Trans. Microw. Theory Techn.*, vol. 58, no. 12, pp. 4040–4051, Dec. 2010, doi: 10.1109/TMTT.2010.2083682.

[12] G. Fischer, O. Klymenko, D. Martynenko, and H. Luediger, "An impulse radio UWB transceiver with high-precision TOA measurement unit," in *Proc. Int. Conf. Indoor Position. Indoor Navig.*, 2010, pp. 1–8, doi: 10.1109/IPIN.2010.5647785.

[13] H. Viswanathan and P. E. Mogensen, "Communications in the 6G era," *IEEE Access*, vol. 8, pp. 57063–57074, 2020, doi: 10.1109/ACCESS.2020.2981745.

[14] C. De Lima et al., "Convergent communication, sensing and localization in 6G systems: An overview of technologies, opportunities and challenges," *IEEE Access*, vol. 9, pp. 26902–26925, 2021, doi: 10.1109/ACCESS.2021.3053486.

[15] A. F. Molisch, "Ultra-wide-band propagation channels," *Proc. IEEE*, vol. 97, no. 2, pp. 353–371, Feb. 2009, doi: 10.1109/JPROC.2008.2008836.

[16] M. A. T. Sanduleanu and J. R. Long, "CMOS integrated transceivers for 60GHz UWB communication," in *Proc. IEEE Int. Conf. Ultra-Wideband*, 2007, pp. 508–513, doi: 10.1109/ICUWB.2007.4380998.

[17] S. Goto et al., "Stability analysis and layout design of an internally stabilized multi-finger FET for high-power base station amplifiers," in *IEEE MTT-S Int. Microw. Symp. Dig.*, vol. 1, 2003, pp. 229–232, doi: 10.1109/MWSYM.2003.1210922.

[18] Y. T. Chan and K. C. Ho, "A simple and efficient estimator for hyperbolic location," *IEEE Trans. Signal Process.*, vol. 42, no. 8, pp. 1905–1915, Aug. 1994, doi: 10.1109/78.301830.

MICHAEL BOCQUET received the Ph.D. degree in electronics engineering and telecommunications from the University of Sciences and Technologies, Lille, France, in 2007.

He worked as a Radio Engineer with INRETS (currently Gustave Eiffel University), Champs-sur-Marne, France, in 2008. In 2009, he joined the Institut d'Electronique, de Microélectronique et de Nanotechnologies, Université de Lille, CNRS, Université Polytechnique Hauts-de-France, UMR 8520-IEMN, Lille, France, where he is currently an Assistant Professor. His main research activities are RF transceivers for telecommunications, localization systems operating in millimeter-wave frequency bands, and wireless sensor networks. In this domain, he studied networks of wireless sensors for the nondestructive test of rails and for the energy efficiency inside railway vehicle.

NATHALIE ROLLAND received the Engineering degree in microelectronics from Polytech'Lille, University of Lille, Villeneuve-d'Ascq, France, in 1986, and the Ph.D. degree in electronics and the HDR degree from the University of Lille, Villeneuve-d'Ascq, in 1989 and 2002, respectively.

She is currently a Professor with the Engineer School Polytech'lille, University of Lille. She is the Head of the IRCICA CNRS Laboratory (Research institute on Hardware-software devices for Advanced Information and communication, CNRS, and University of Lille). Since 2000, she has been mainly involved in the field of advanced communication systems for smart object communication and sensors networks.

CHRISTOPHE LOYEZ (Member, IEEE) received the M.Sc. and Ph.D. degrees from the University of Lille, Villeneuve-d'Ascq, France, in 1996 and 2000, respectively.

He is the CNRS Research Director of the Institut d'Electronique, de Microélectronique et de Nanotechnologies, Université de Lille, CNRS, Université Polytechnique Hauts-de-France, UMR 8520-IEMN, Lille, France. He has initiated several multidisciplinary research activities on high-speed wireless systems and low-power systems for radio-communication and localization. He is regularly the Scientist in charge of projects on millimeter-wave systems and integrated RF systems. He has been accredited to Direct Research (HDR) since 2012 and is the Thesis Supervisor on energy efficiency systems. Since 2015, he has been the Leader of the Circuits & Systems for Applications of Microwaves Research Group, composed of more than ten researchers, whose research activities concern the energy efficiency of transmission and information processing systems. A member of the organizing committee of the French chapter of the IEEE Solid State Circuit, he is also a Co-Leader of the joint laboratory e-COST "Enhanced Communication Devices for Smart Cities and Transports," which brings together more than 20 researchers from IEMN and the Gustave Eiffel University, Champs-sur-Marne, France, on topics related to smart cities and transport.

KAMEL HADDADI (Member, IEEE) received the M.S. and Ph.D. degrees from the University of Lille, Villeneuve-d'Ascq, France, in 2003 and 2007, respectively.

He is currently a Full Professor with the Institute of Electronics, Microelectronics and Nanotechnology, joint research unit between the University of Lille and the CNRS. His research activities are the development of RF measurement techniques and systems for microwave Non-Destructive Testing & Evaluation (NDT&E) purposes. The results achieved in this context led to publication of around 100 articles in peer review international papers and conferences.

Prof. Haddadi is a member of the international committees IEEE MTT-S TC-8 RF Nanotechnology and MTT-S TC-24 MICROWAVE/MM-WAVE RADAR, SENSING AND ARRAY SYSTEMS, an Associate Editor of IEEE TRANSACTIONS ON INSTRUMENTATION AND MEASUREMENT and a TPC member in various IEEE conferences.